

## Supporting information

### **Hydrogen-terminated mesoporous silicon monoliths with huge surface area as alternative Si-based visible light-active photocatalysts**

Ting Li,<sup>†</sup> Jun Li,<sup>‡</sup> Qiang Zhang,<sup>‡</sup> Emma Blazeby,<sup>†</sup> Congxiao Shang,<sup>&</sup> Hualong Xu,<sup>§</sup> Xixiang Zhang,<sup>‡</sup> and Yimin Chao<sup>\*,†</sup>

<sup>†</sup>School of Chemistry, University of East Anglia, Norwich Research Park, Norwich, NR4 7TJ, United Kingdom

<sup>‡</sup> King Abdullah University of Science and Technology (KAUST), Division of Physical Science and Engineering, Thuwal 23955, Saudi Arabia

<sup>&</sup>School of Environmental Sciences, University of East Anglia, Norwich, NR4 7TJ, United Kingdom

<sup>§</sup>Department of Chemistry, Shanghai Key Laboratory of Molecular Catalysis and Innovative Materials and Laboratory of Advanced Materials, Fudan University, Shanghai 200433, P. R. China

[\\*Y.Chao@uea.ac.uk](mailto:Y.Chao@uea.ac.uk)

**1. Cross sectional SEM images of various mesoporous silicon samples (JEOL JSM 5900 LV model fitted with a Tungsten filament and acceleration voltage used was 20 kV)**

The uniformity of the layer thickness was commonly featured in a variety of porous silicon samples and it increases with etching time and external current density.

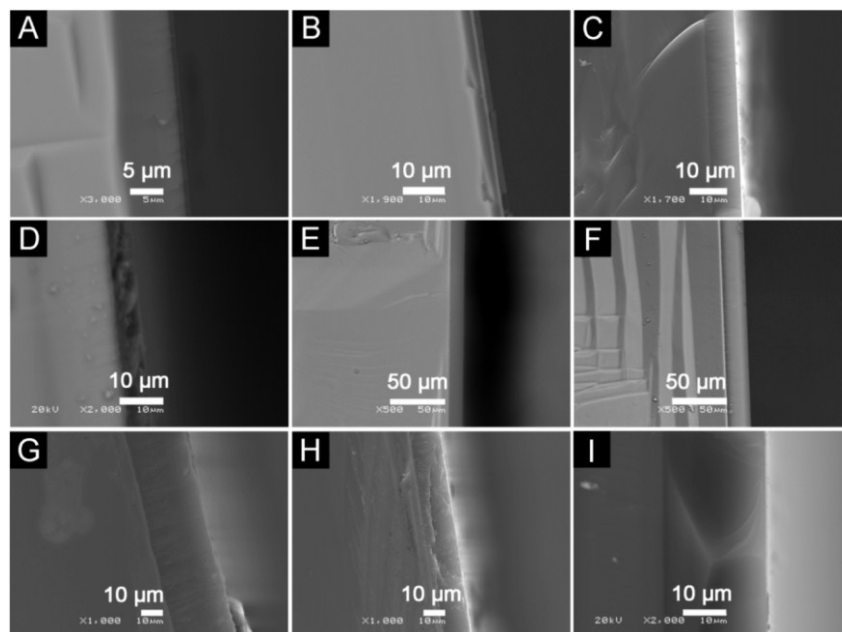


Fig. S1 Cross sectional SEM micrographs of (A) I-MPSi-10-02, (B)I-MPSi-10-05, (C) I-MPSi-10-15, (D) I-MPSi-10-25, (E) I-MPSi-10-30, (F) I-MPSi-10-35, (G) I-MPSi-10-40, (H) I-MPSi-60-05, (I) I-MPSi-60-15, respectively.

Samples	Etching current density / mA·cm <sup>-2</sup>	Etching time / min
I-MPSi-10-02	10	02
I-MPSi-10-05	10	05
I-MPSi-10-15	10	15
I-MPSi-10-25	10	25
I-MPSi-10-30	10	30
I-MPSi-10-35	10	35
I-MPSi-10-40	10	40
I-MPSi-60-05	60	05
I-MPSi-60-15	60	15

2. The cross sectional FE-SEM images of I-MPSi-30 and O-MPSi-150 (Tilt 45°) showing the general top-down texture, although this may be obscured by artificial defects from sample cleaving.

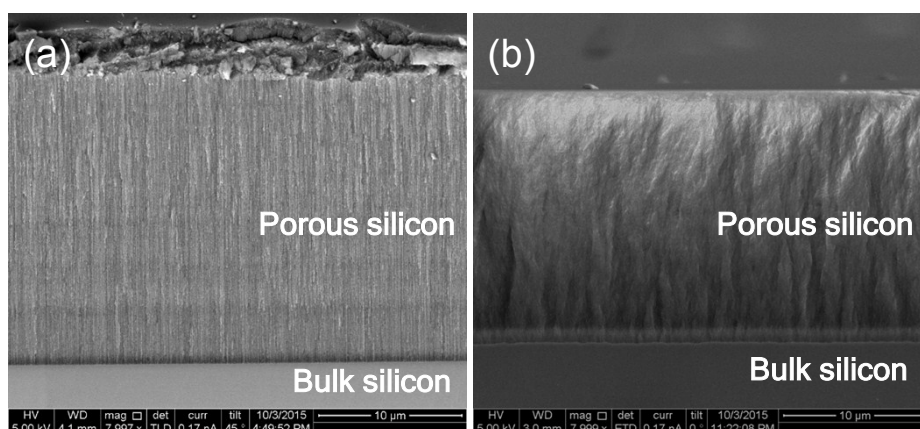


Fig. S2 Cross sectional FESEM micrographs of O-MPSi-150 (a) and I-MPSi-30 (b)

### 3. Nitrogen sorption isotherms

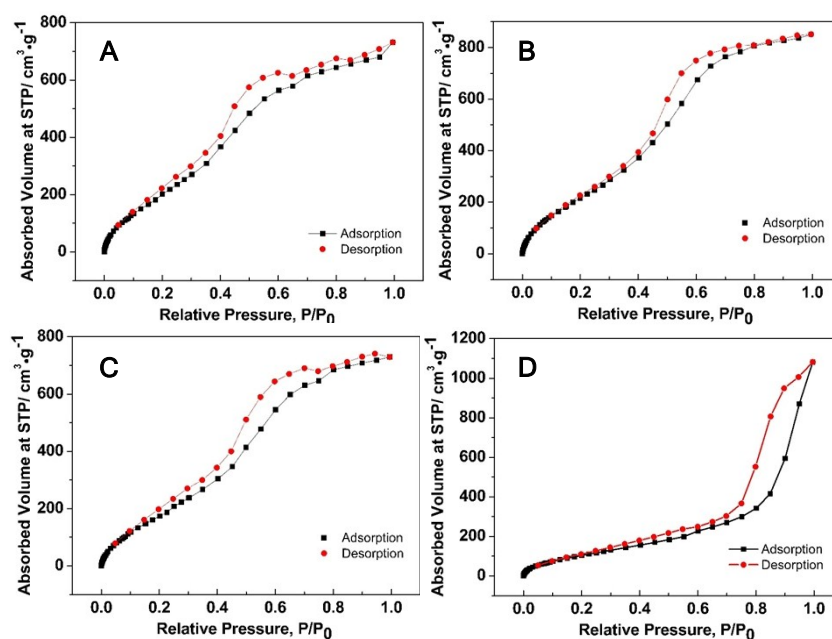


Fig. S3 Nitrogen adsorption-desorption isotherms (adsorption branch (■) and desorption branch (●)) measured on I-MPSi-10(A), I-MPSi-60(B), I-MPSi-60-05(C) and O-MPSi-150-10 (D), respectively. The formation conditions can be referred to Table 1.

#### 4. The control experiments in the MO degradation test

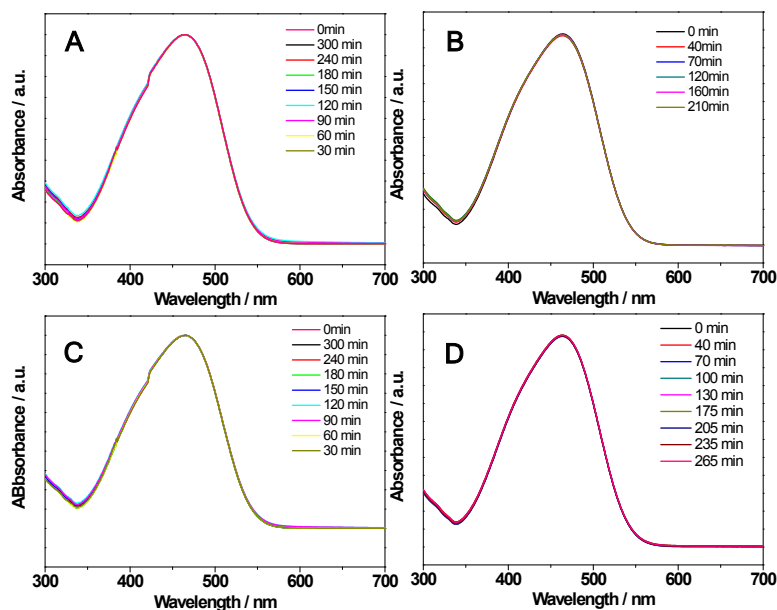


Fig. S4 UV-Vis absorption of methyl orange at different time intervals of reaction using different Si chips: (A) moderately doped p-type Si chip under visible light irradiation; (B) moderately doped p-type Si chip in the dark; (C) methyl orange solution under visible light irradiation; (D) heavily doped p-type Si chip under visible light irradiation. An 8W fluorescent lamp was used. The initial MO concentration is  $5.0 \times 10^{-5}$  M.

#### 5. IR spectra of mesoporous silicon at different intervals of the reaction

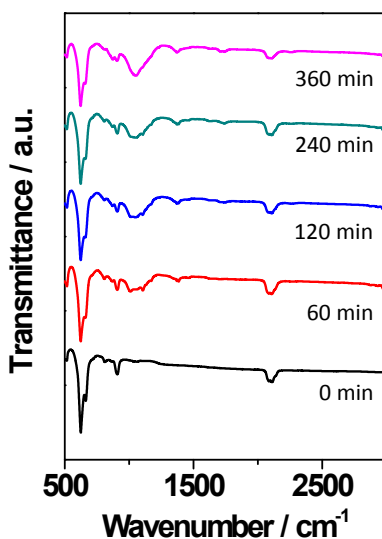


Fig. S5 The IR spectra of I-MPSi-30 at 0 min, 60 min, 120 min, 240 min, 360 min intervals, during the reaction. The initial MO concentration is  $5.0 \times 10^{-5}$  M.

## 6. IR spectra of surface oxidized mesoporous silicon samples

Experiment procedure:

I-MPSi-30 and O-MPSi-150 were dipped into 10 w.t. % hydrogen peroxide dilute solution. Thereafter they were rinsed with ethanol and dried under vacuum overnight.

After the hydrogen peroxide treatment, the surfaces of mesoporous silicon samples were completely oxidized and covered by a thin layer of silicon oxides with the presence of the intensive absorption at  $1050\text{ cm}^{-1}$  from Si-O-Si in the IR spectra. At the same time, Si-H<sub>x</sub> signals ( $2087, 2100, 2139\text{ cm}^{-1}$ ) no longer appeared while the  $615\text{ cm}^{-1}$  Si-Si bond was still observed which represents the preserved silicon structure after the surface oxidation.

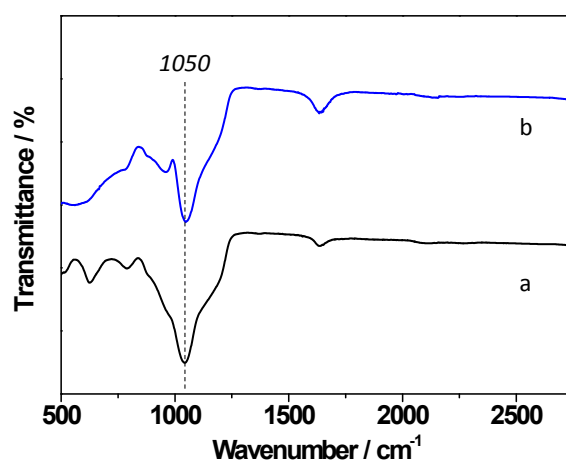


Fig. S6 IR spectra of surface oxidized mesoporous silicon samples: (a) O-MPSi-150; (b) I-MPSi-30

## 7. Physical absorption of methyl orange by the surface oxidized mesoporous silicon samples

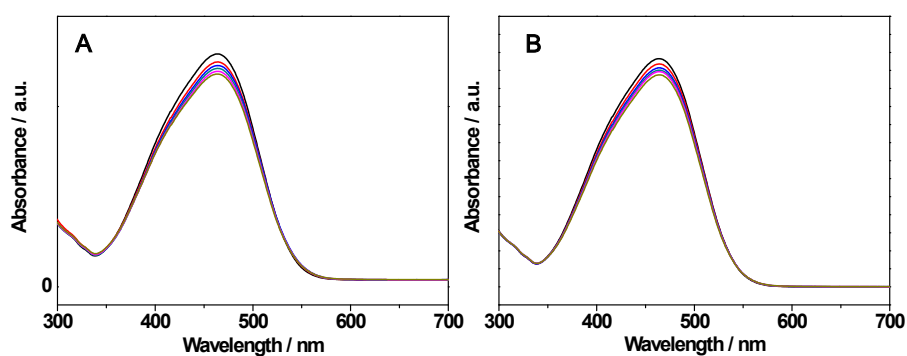


Fig. S7 Dye absorption results of the surface oxidized samples: (A) O-MPSi-150; (B) I-MPSi-30. The initial MO concentration is  $5.0 \times 10^{-5}\text{ M}$ .

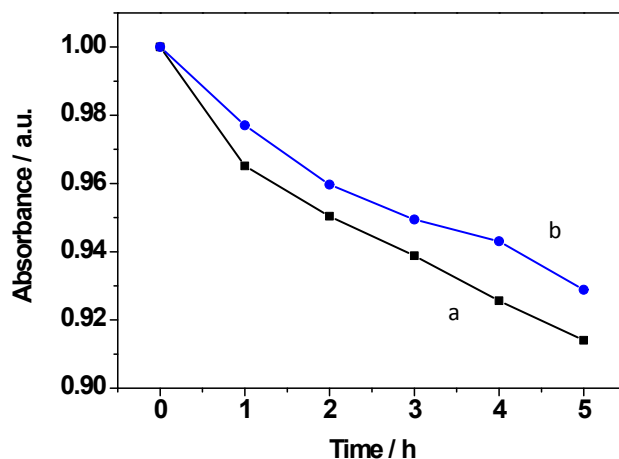


Fig. S8 The UV-Vis absorbance of MO residues without being absorbed physically by surface oxidized samples: O-MPSi-150 (a) and I-MPSi-30 (b) for 1h, 2hs, 3hs, 4hs, and 5hs.

## 8. TOC analysis

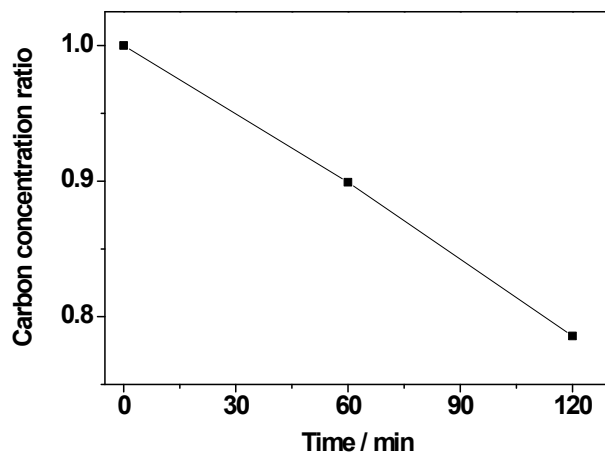


Fig. S9 The total organic carbon content in the MO solution in the presence of O-MPSi-150 under visible light irradiation for 0 min, 60 min and 120 min.

## 9. UV-Vis absorption spectrum of O-MPSi-200 and its MO degradation results

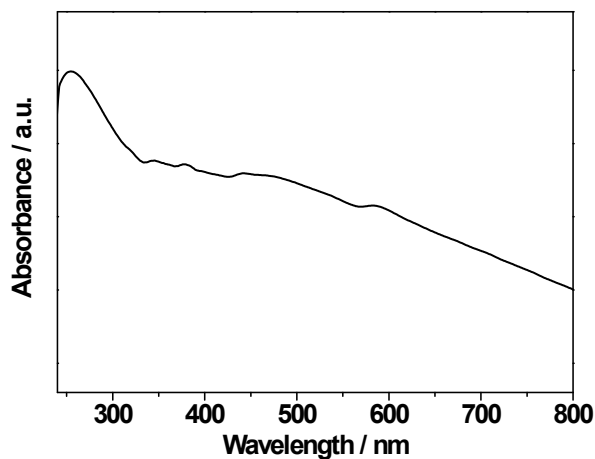


Fig. S10 The UV-Vis absorption spectrum of O-MPSi-200

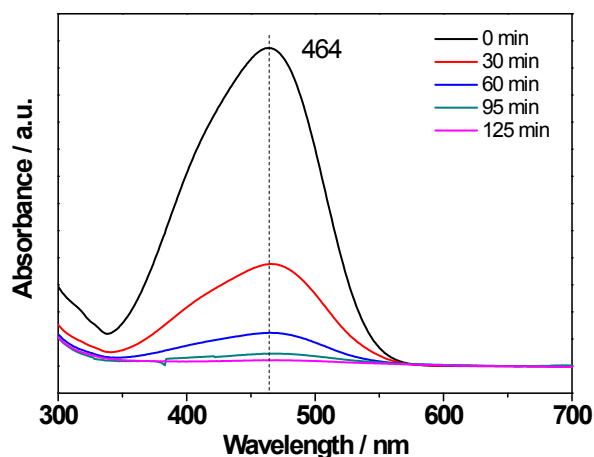


Fig. S11 UV-Vis absorption of methyl orange at different time intervals in the presence of O-MPSi-200 under visible light irradiation. An 8W fluorescent lamp was used. The initial MO concentration is  $5.0 \times 10^{-5}$  M.

## 10. ATR-IR spectra of mesoporous silicon microparticles and their MO degradation results

Preparation:

At the end of the electrochemical etching, the ‘lift-off’ treatment was applied to samples by a sudden increase of the etching current density for a few seconds. Thereafter followed by drying under vacuum for several hours they were quickly transferred into 20 mL dry dichloromethane (DCM) and sonicated under nitrogen flow for 30 min in an ice bath. Then after the solvent was removed by pumping, free standing porous silicon microparticles were successfully obtained.

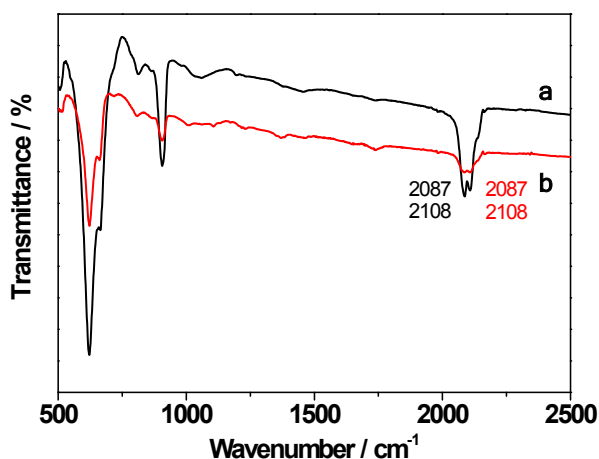


Fig. S12 ATR-IR spectra of as prepared I-MPSi-30 particles (a) and O-MPSi-200 particles (b)

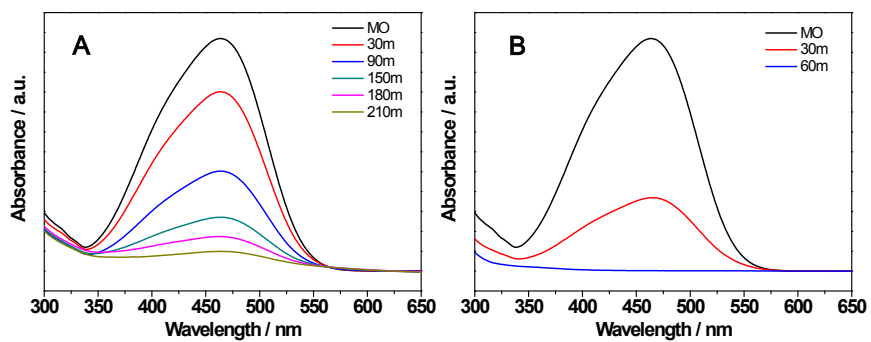


Fig. S13 The MO degradation results of hydrogen passivated I-MPSi-30 particles (A) and O-MPSi-200 particles (B). An 8W fluorescent lamp was used. The initial MO concentration is  $5.0 \times 10^{-5}$  M.